

Original Research Paper

Water Filter Fabrication from a Mixture of KMnO_4 Modified Kapok Carbon Fiber, Zeolite, Bentonite and Clay for Fe^{3+} Removal and Water Hardness Treatment

Kannika Thongdee, Kalayaporn Parun,
Suphakrit Benjatitmongkhon, Krit Jamtim and Sumrit Mopoung*

Department of Chemistry, Faculty of Science, Naresuan University, Phitsanulok, Thailand

Article history

Received: 08-12-2016

Revised: 01-06-2017

Accepted: 07-06-2017

Corresponding authors

Sumrit Mopoung

Department of Chemistry,
Faculty of Science, Naresuan
University, Phitsanulok,
Thailand

Email: sumritm@nu.ac.th

Abstract: A water filter was fabricated from a mixture of KMnO_4 modified kapok carbon fiber, zeolite, bentonite and kaolinite clay for Fe^{3+} removal and water hardness treatment. The effects of amount of KMnO_4 modified kapok carbon fiber (30-60 wt%), zeolite (20-40 wt%) and sintering temperature (500-700°C) on the properties of sintered products were evaluated. The best of sintered products were tested for treatment of solutions with 5 mg L^{-1} Fe^{3+} and 40-200 mg L^{-1} total water hardness. The results show that the physical properties of the sintered products were affected by the contents of KMnO_4 modified kapok carbon fiber and sintering temperature. The linear drying shrinkages of the mixture of raw materials increase with increasing content of modified kapok carbon fiber amounts due to the effect of water amount used for mixing process. Furthermore, firing shrinkages of sintered products increased with increasing sintering temperature for the same ratio of raw materials. Finally, the firing shrinkages and density of sintered products decrease with increasing content of the modified kapok carbon fiber at constant sintering temperature. It was shown that the sintered product made with 40 wt% of KMnO_4 modified kapok carbon fiber and sintered at 600°C is suitable for filter fabrication. The KMnO_4 modified kapok carbon fiber filter could adsorb 5-6% more Fe^{3+} at equilibrium than filter made with kapok carbon fiber. The Fe^{3+} was removed by adsorption and precipitation processes. The Fe^{3+} adsorption process of modified kapok carbon fiber filter was fitted to the Langmuir model with maximum adsorption capacity of 53.76 mg g^{-1} . For hardness removal, the Ca^{2+} , Mg^{2+} and HCO_3^- ions removal capacities from solutions of total hardness in the range 40-200 mg L^{-1} by modified kapok carbon fiber filter are 4.49-19.21 mg g^{-1} for Ca^{2+} , 1.55- 5.31 mg g^{-1} for Mg^{2+} and 28.1-123.5 mg g^{-1} for HCO_3^- , respectively.

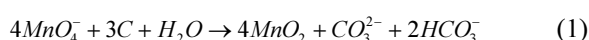
Keywords: Water Filter, Fe^{3+} , Hardness Water, KMnO_4 Modified Kapok Carbon Fiber, Clay Minerals

Introduction

Porous ceramics have been widely used for separation applications where they are valued for their thermal resistance, structural stability and mechanical strength (van Garderen *et al.*, 2011). Meanwhile, activated carbon has also been widely used as an adsorbent for the removal of organic and inorganic pollutants from water and wastewater. The application of activated carbon in adsorption processes mainly depends on its surface chemistry and pore structure (Bhatnagar *et al.*, 2013).

Thus, it can be added to clay minerals for carbon-based porous ceramics production. Carbon-mineral adsorbents have been prepared using clay minerals and these adsorbents have also been applied in purification of water and sewage (Leboda *et al.*, 2001). For activated carbon, the method of activation and the nature of the precursor greatly influence surface functional groups and pores structure of the activated carbon product (Bhatnagar *et al.*, 2013). Potassium permanganate is a substance that has been used for activation of carbon and water treatment (Han *et al.*, 2013). It is widely used in

water treatment processes where strong oxidants are utilized for degradation of various organic pollutants, e.g., steroid estrogens, oxytetracycline etc. (Fang *et al.*, 2016). Furthermore, the use of KMnO_4 can aid the removal of iron and/or manganese, or algae (Lin *et al.*, 2012). KMnO_4 oxidation has been combined with polyelectrolyte flocculation to mitigate membrane fouling in membrane bioreactors. It has been shown to reduce the COD value in the effluent more than procedures omitting the use of KMnO_4 flocculants (Zarei-Baygi *et al.*, 2016). KMnO_4 preoxidation produces fewer by-products in the treatment of raw water. Permanganate ion (MnO_4^-) from KMnO_4 is transformed into MnO_2 by the redox reaction in presence of C and water as shows in Equation 1 (Mu *et al.*, 2015):



The hydrated manganese dioxide usually exists as a colloid or a suspended solid in aqueous medium. It has a large surface area with strong adsorptive capacity, which can adsorb CaCO_3 and CaSO_4 that are then retained on the membrane surface to form a loose filter cake (Lin *et al.*, 2012). It can also get accumulated on surface of many substances (Fang *et al.*, 2016). Fabrics containing immobilized manganese oxides have also been developed for the removal of ozone, formaldehyde and arsenic. These fabrics have been produced by radiation induced graft polymerization and applied for the purification of contaminants in environment (Fujiwara *et al.*, 2010). The use of KMO_4 also increases environmental friendliness of a process by avoiding formation of chlorinated disinfection by-products and bromate in chlorination and ozonation processes (Han *et al.*, 2013). It can reduce the hydrophilicity of the membrane to aggravate membrane fouling and increase the hydrophilicity of organic matter to membrane fouling (Lu *et al.*, 2015). It has also been used for sand filter effluent pretreatment and performance in combined ultra filtration processes. It shows significant improvements to the efficiency of natural organic matter removal. Furthermore, it can oxidize metal ions into metal oxide particles, which are adsorbed on the membrane surface together with the pollutants. The MnO_2 nanowires-deposited diatomite samples have been prepared using the hydrothermal method with KMnO_4 and $(\text{NH}_4)_2\text{S}_2\text{O}_8$. These MnO_2 nanowires/diatomite samples showed high surface areas and good Cr^{4+} and As^{3+} adsorption behaviors (Du *et al.*, 2014). The hollowed-out tubular carbon/ MnO_2 hybrid composites with hierarchical morphology have been prepared via the redox reaction between MnO_4^- and tubular carbonized kapok (Mu *et al.*, 2015). MnO_2 nanostructures have also been successfully coated onto activated mesocarbon microbeads by a simple chemical co precipitation method (Li *et al.*, 2010). Furthermore, conductive MnO_2 /reduced graphene oxide/carbon was prepared by carbonization of MnO_2 /graphene oxide on

cotton. It contains a large amount of oxygenous groups, which could be useful to uniformly deposit graphene oxide nanosheets and MnO_2 nanoparticles (Tian *et al.*, 2016). Woody biomass (pine chips) have been treated with permanganate to enhance the heavy metal sorption capacity by increasing the carboxylic ($-\text{COOH}$) surface group content (McLaughlan *et al.*, 2015). Moreover, KMnO_4 could also oxidize carbon based materials to exhibit the hydroxyl ($-\text{OH}$) and carbonyl ($\text{C}=\text{O}$) groups on the surface (Rasheed *et al.*, 2007).

Lignocellulosic agricultural byproducts are a vast and cheap source of cellulose fibers, which have the composition, properties and structure that make them suitable for uses such as composite, textile, pulp and paper manufacture. In addition, they can also be used to produce fuel, chemicals, enzymes and food (Reddy and Yang, 2005). The kapok fiber is one of agricultural products, which has a very thin cell wall with a huge hollow region full of air (Mu *et al.*, 2015), low density, good buoyancy and excellent hydrophobicity. It is a highly lignified organic seed fiber and mainly consists of cellulose, lignin and xylan (Zheng *et al.*, 2015). The surface of kapok fiber is smooth with a thick layer of wax. The cross-section is oval to round with large lumen and thin wall (ca. 8-10 μm in diameter and ca. 0.8-1.0 μm in wall thickness). It has a porosity of more than 80% (Zheng *et al.*, 2015) and it is fluffy with a bulk density of 0.305 g/cm^3 (Dong *et al.*, 2015a). Kapok fiber exhibits high hydrophobic-oleophilic characteristics, attributed to its hollow lumen and its waxy surfaces. It is abundant, biocompatible and biodegradable and its exploration for potential applications increased in both academic and industrial fields. It has also been applied as an absorbent material for metal ions, dyes and sound (Zheng *et al.*, 2015). It was modified by coating with the mixture of polybutylmethacrylate and hydrophobic silica (SiO_2) (Wang *et al.*, 2013) and by silica nanoparticles via solgel method and subsequent hydrophobic modification using hydrolyzed dodecyltrimethoxysilane (Wang *et al.*, 2012). The resultant materials exhibited excellent oil/water selectivity in the cleanup of oil over water. It showed high oil sorption capacity, excellent hydrophobic properties, reusability and good environmental friendliness. It has been also oxidized by steam (Chung *et al.*, 2013) and sodium chlorite (NaClO_2) (Liu *et al.*, 2012) for the removal of methylene blue from aqueous solutions. This oxidized material showed high surface area and large hollow pore volume. Furthermore, Fe_3O_4 nanoparticles have been immobilized on its surface, which was followed by hydrophobic modification. The resultant material demonstrated excellent superhydrophobicity and magnetic properties with high separation efficiency for oil/water mixtures. It can quickly absorb floating oils on water surface using magnetic driving (Wang *et al.*, 2016).

Clay minerals, such as montmorillonite, bentonite, attapulgite, vermiculite, illite, sericite and kaolinite have been used as adsorbents for metals (Pawar *et al.*, 2016), toxins and waste material (Tahir and Naseem, 2007).

Their major constituents are SiO₂ and Al₂O₃. Their structure usually contains a tetrahedral silicon oxide layer with some silicon atoms replaced with trivalent cations, sandwiched between two octahedral aluminium oxide layers with some aluminum atoms replaced with divalent cations. Therefore, it is expected that either SiO₂ or Al₂O₃ present in the adsorbent or their combined influence are likely to be responsible for the adsorption of metal ions (Tahir and Naseem, 2007) as their negative charge (generated by isomorphous substitution of Si⁴⁺ by Al³⁺) is counterbalanced by native cations (Na⁺, K⁺, Ca²⁺ and Mg²⁺) and water molecules in their pores and channels (Koshy and Singh, 2016). Bentonite is the best adsorbent with high cation exchange capacity, high specific surface area, excellent physical and chemical stability and surface properties (Pawar *et al.*, 2016). It also has good sorption characteristics with respect to heavy metals. Features of its structure create the possibility of sorption of heavy metals on the external surface of the particles and in the interlayer spacing of the structural layers with substitution of the appropriate ion-exchange positions (Sultanbayeva *et al.*, 2013). It has been found beneficial for pollution control applications (Tahir and Naseem, 2007). Zeolite also has a high adsorption activity and typical molecular sieve properties. It is also used as water softener (Loiola *et al.*, 2012). However, it was used in combination with bentonite for increasing sedimentation of the composite sorbent. Thus, porous structure, good physical and chemical characteristics and low costs of zeolite and bentonite allow extensive use of these sorbents as ion exchangers, catalysts etc. (Sultanbayeva *et al.*, 2013). Kaolinite clay has high chemical stability, cation exchange capacity and low expansion coefficient. Its structure is also a tetrahedral silica sheet alternating with an octahedral alumina sheet (Uddin, 2017). It was used as a binding agent since the clay itself has binding and adsorption capacity and can increase reinforcement of the adsorbent (Boonamnuyvitaya *et al.*, 2004).

Iron is abundant element of the earth's crust which can contaminate groundwater. Although iron is an essential mineral for humans, its presence in groundwater above a certain level makes the water unusable mainly for aesthetic considerations such as discoloration, metallic taste, odor, turbidity and staining of laundry (Chaturvedi and Dave, 2012). Hardness is also an issue found in groundwater related to the presence of calcium and magnesium. Hard water, for example, leads to the formation of soap scum when soap is mixed with water, which necessitates the use of more soap for cleaning purposes (Morales-Pinzón *et al.*, 2014).

In this research, the KMnO₄ modified kapok carbon fiber was used to improve properties of porous ceramics. The porous ceramics are fabricated from KMnO₄ modified kapok carbon fiber, zeolite, bentonite, kaolinite clay and borax as fluxing reagent. The effects of KMnO₄ modified kapok carbon fiber and zeolite content and sintering temperature are investigated in order to improve

the properties of the porous ceramic materials such as drying shrinkage, firing shrinkage, density, morphology and removal efficiency of Fe³⁺ and water hardness treatment.

Materials and Methods

Preparation of KMnO₄ Modified Kapok Carbon Fiber

The kapok fiber was obtained from Phitsanulok province, Thailand. It was separated from the kapok fruit cob and then dried in an oven (SL 1375 SHEL LAB 1350 FX, USA) at 110°C for 3 h. The dried kapok fiber was carbonized at 500°C in an electric furnace (Fisher Scientific Isotemp® Muffle Furnace) for 30 min. After carbonization, the kapok carbon fiber was soaked with 1 wt% KMnO₄ (Merck, Germany) dissolved in water and then dried at 110°C for 3 h. The dried product is KMnO₄ modified kapok carbon fiber.

Preparation of Porous Ceramic Materials

Zeolite (commercial grad), bentonite (commercial grad) and kaolinite clay (obtained from Lampang province, Thailand) were ground, sieved (Laboratory test sieve, Retsch, Germany) to 60 mesh and dried at 110°C for 3 h. All of these raw materials were mixed with KMnO₄ modified kapok carbon fiber. The ratios, by weight, of KMnO₄ modified kapok carbon fiber:zeolite:bentonite:kaolin clay:borax, which is shown in Table 1, were used for the fabrication of the porous ceramic materials. All mixtures are wetted with water and pressed in PVC tube (length = 50 mm and diameter = 12.70 mm). The wetted products were dried in an oven at 110°C for 3 h and then sintered under reducing conditions (placed in a box closed by a flip) in an electric furnace at 500, 600°C and 700°C for 30 min. The linear drying shrinkage, linear firing shrinkage and density of wetted products and sintered products were measured. The SEM (LEO 1455 VP) was also used for characterization of kapok carbon fiber, KMnO₄ modified kapok carbon fiber and selected sintered products. The best sintered product was used for Fe³⁺ and hardness removal experiments.

The Adsorption Experiments

Fe³⁺ Adsorption Experiment

Batch Fe³⁺ adsorption experiments were performed using the method of Üçer *et al.* (2005). The effect of contact time (0-180 min) was investigated using 0.1 g sintered filter in 50 mL of 5 mg L⁻¹ Fe³⁺ solutions at pH 7±0.15 by shaken continuously at 120 rpm and a temperature of 32±2°C in a conical flask to achieve optimum performance of Fe³⁺ adsorption. The pH 7 was used for Fe³⁺ adsorption experiments following the protocol GB5033522002 of Wastewater Reclamation and Reuse Engineering Design Standards for reused water quality (Xuwen *et al.*, 2010).

Table 1. The ratios (wt%) of raw materials for porous ceramic materials fabrication

Number	Modified carbon fiber	Zeolite	Bentonite	Kaolinite clay	Borax
1	60	20	10	10	0
2	40	30	10	10	10
3	30	40	10	10	10
4	50	20	10	10	10

For adsorption isotherm experiments, the sintered filters (0.05, 0.1, 0.5, 1.0, 1.5, 2.0 g) were also added to 50 mL of 5 mg L⁻¹ Fe³⁺ solutions at pH 7±0.15 in conical flasks and shaken continuously at 120 rpm at a temperature of 32±2°C for 60 min. Following the adsorption, the aqueous phases were separated by centrifugation at 4000 rpm for 10 min and the final concentrations of Fe³⁺ ion in the solutions were determined by FAAS (Varian SpectraAA 220, Australia) with air-acetylene and cathode on Fe-hollow cathode lamp at 248.3 nm.

The amounts of adsorbed Fe³⁺ ions were calculated by the difference in initial and final concentrations.

Adsorption Isotherms

All of the experimental adsorption data were fitted with both the Langmuir equation and the Freundlich equation.

The rearranged Langmuir equation is as follows (Mopoung and Amornsakchai, 2016):

$$Q_e = (Q_{\max} K_L C_e) / (1 + K_L C_e) \quad (2)$$

where, Q_e (mg g⁻¹) is the amount of Fe³⁺ adsorbed per unit mass of adsorbent, C_e (mg L⁻¹) is the Fe³⁺ equilibrium concentration, Q_{\max} (mg g⁻¹) is the maximum Fe³⁺ amount that forms a complete monolayer on the surface and K_L (L mg⁻¹) is the Langmuir constant related to adsorption heat. The linear form of this equation after rearrangement is as follows (Mopoung and Amornsakchai, 2016):

$$C_e / Q_e = (1 / Q_{\max} K_L) + C_e / Q_{\max} \quad (3)$$

The constants Q_{\max} and K_L can be determined from the slope and intercept of plotting C_e / Q_e against C_e , respectively.

The Freundlich model is used to estimate the adsorption intensity of filter towards the Fe³⁺ ion and the equation is as follows (Mopoung and Amornsakchai, 2016):

$$Q_e = K_F C_e^{(1/n)} \quad (4)$$

This equation is conveniently used in linear form as (Mopoung and Amornsakchai, 2016):

$$\log Q_e = \log K_F + 1/n \log C_e \quad (5)$$

where, Q_e and C_e have the same definitions as those in the Langmuir equation cited above. K_F and n are Freundlich constants related to adsorption capacity and heterogeneity factor, respectively. The constants K_F and n can also be determined from the intercept and slope of plotting $\log C_e$ against $\log Q_e$, respectively.

Hardness Adsorption Experiments

Hardness adsorption experiments were performed following the method of Pastrana-Martínez *et al.* (2010). Solutions for this experiment were prepared using distilled water with varied degrees of hardness and alkalinity. Total hardness and alkalinity were calculated according to Equation 6 and 7, respectively:

$$\begin{aligned} \text{Total hardness as CaCO}_3 \text{ (mg L}^{-1}\text{)} \\ = 2.50 [\text{Ca}^{2+}; \text{mg L}^{-1}] + 4.12 [\text{Mg}^{2+}; \text{mg L}^{-1}] \end{aligned} \quad (6)$$

$$\begin{aligned} \text{Total alkalinity as CaCO}_3 \text{ (mg L}^{-1}\text{)} \\ = 0.82 [\text{HCO}_3^-; \text{mg L}^{-1}] + 1.67 [\text{CO}_3^{2-}; \text{mg L}^{-1}] \end{aligned} \quad (7)$$

Waters with hardness values of 40, 100, or 200 mg L⁻¹ CaCO₃ were prepared by using CaCl₂, MgCl₂ and NaHCO₃ (Merck, Germany) dissolved in distilled water. Hardness values of 40, 100 and 200 mg L⁻¹ CaCO₃ correspond to soft, moderately hard and hard water, respectively. The pH of the synthetic and tap waters was between 8.0 and 8.7; according to the speciation diagram of the carbonate-bicarbonate system, only the bicarbonate ion is present at this pH range. Concentrations of HCO₃⁻, Ca²⁺ and Mg²⁺ for the 40 mg L⁻¹ hardness and 46 mg L⁻¹ alkalinity are 56.2, 9.7 and 3.9 mg L⁻¹ respectively. The concentrations for the same species for 100 mg L⁻¹ hardness and 101 mg L⁻¹ alkalinity are 123.5, 24.2 and 9.5 mg L⁻¹ respectively. Finally, for 200 mg L⁻¹ hardness and 202 mg L⁻¹ alkalinity, the concentrations are 247.0, 48.0 and 19.1 mg L⁻¹ respectively. HCO₃⁻ concentrations were determined by titration with 0.1 N HCl (Pastrana-Martínez *et al.*, 2010). Ca²⁺ and Mg²⁺ concentrations were determined by FAAS with 427.7 nm and 285.2 nm, respectively (Lyra *et al.*, 2010).

Removal Efficiency of Fe^{3+} , Ca^{2+} , Mg^{2+} and HCO_3^- ions

Final concentrations (C_f) of Fe^{3+} , Ca^{2+} , Mg^{2+} , or HCO_3^- ions were measured for the calculation of removal percentages of Fe^{3+} , Ca^{2+} , Mg^{2+} and HCO_3^- ions as shown in Equation 8 (Hajji *et al.*, 2016):

$$\text{Removal efficiency} = \left[\frac{(C_o - C_f)}{C_o} \right] \times 100 \quad (8)$$

where, C_o is the initial concentration of the given ion ($mg L^{-1}$) and C_f is the final concentration of the same species ($mg L^{-1}$). The adsorption capacity (q_t , $mg g^{-1}$) at any time was calculated using a mass balance equation as shown in the Equation 9 (Hajji *et al.*, 2016):

$$q_t = (C_o - C_f) \times (V/W) \quad (9)$$

Results and Discussion

The Physical Properties of Wetted Materials and Sintered Products

Based on Table 2, the linear drying shrinkage percentage of a mixture raw materials increase (4.13-4.63%) with increasing content of modified kapok carbon fiber (30-60 wt%, number 3 \rightarrow 2 \rightarrow 4 \rightarrow 1). The increasing drying shrinkage is due to the increasing water amount, which was used for mixing (Bouziadi *et al.*, 2016). A high amount of water must be added during shaping to achieve comparable plasticity (Bories *et al.*, 2015) of a mixture of raw materials when high content of modified carbon fiber material is used. Therefore, the swelling behaviour of a mixture of raw materials increases with increasing water content (Kinuthia and Oti, 2012). This is because drying shrinkage takes place due to moisture loss. Thus, the drying shrinkage increases with increasing moisture loss (Ye and Radlińska, 2016). The firing shrinkage percentages of sintered products increase with increasing sintering temperature for the same ratio of raw materials (Table 2). This is due to the effective formation of a liquid phase, which tends to approach the fine pores (Eliche-Quesada *et al.*, 2017). The liquid surface tension and capillarity help to bring particles close together and to enhance firing shrinkages (Monteiro and Vieira, 2004). On the other hand, the firing shrinkage decreases with increasing content of the modified kapok carbon fiber at same sintering temperature. This is due to the enhanced formation of clusters in the mixing stage when higher amounts of modified carbon fiber are used (Vilaplana *et al.*, 2016). The decreasing content of mineral clays in the mixtures of raw materials results in decreasing plasticity of these mixtures, which leads to less contact between the clay particles (Bories *et al.*, 2015). Therefore, the linear firing

shrinkages of sintered products decreased with increasing amounts of the modified kapok carbon fibers. Furthermore, the densities of the sintered products also decreased with increasing content of modified kapok carbon fibers. It is known that the kapok carbon fibers have low density and hollow lumen structure (Zheng *et al.*, 2015). In addition, a portion of the carbon material and volatile compounds present in the mixture of the starting materials are thermally degraded and generate pore volume in matrix materials during sintering (Ukwatta *et al.*, 2016). Therefore, the sintered filters with high content of modified kapok carbon fiber exhibit low density. For 700°C sintering temperature, all of the specimens were not suitable for testing of physical properties because they were severely cracked due to high shrinkage (Bouziadi *et al.*, 2016). Furthermore, the clay minerals usually exhibit extensive shrinkage above 600°C, which can result in cracking and dimensional defects (Bories *et al.*, 2016) in sintered products. In addition, the specimens of sintered products containing 60 wt% of $KMnO_4$ modified kapok carbon fiber were also unsuitable for the testing of physical properties. This is because the mixture of raw materials containing 60 wt% of $KMnO_4$ modified kapok carbon fiber could not maintain the form of the sintered products as it does not have any strong binding materials in the structure (Görhan and Şimşek, 2013). Therefore, the addition of 60 wt% of modified kapok carbon fiber to the raw material mixture leads to much larger defections. On the other hand, the firing shrinkage of the sintered products with 30 wt% of modified kapok carbon fiber is too large for filter fabrication as it destroys the near-net-shaping processing and high porosity (Wu *et al.*, 2016).

Figure 1a and 1b reveals that kapok carbon fiber shows cylindrical hollow lumen structure with a relatively smooth and clean surface containing only minor wrinkles, grooves and cracks. This is attributed to the decomposition of organic materials of kapok fiber during carbonization (Boonamnuyvitaya *et al.*, 2004). The internal diameter and wall thickness of kapok carbon fiber were measured and lie in the range of 5.816-6.497 μm and 460.5-488.7 nm, respectively. When compared to the fresh kapok fiber, which has an average external diameter of 20 μm and relatively smooth surface without any ripples (Dong *et al.*, 2015b), the kapok carbon fiber has shrunk about 4 times after carbonization at 500°C. After modification with $KMnO_4$, small particles were deposited and sparsely attached on the external lumen surface of modified kapok carbon fiber. The subsequent degradation of the carbon on the surface of the fibers generates a new surface more higher wrinkles, grooves and roughness (Fig. 1c). This shows that the $KMnO_4$ reacted with the carbon on the surface of

the fibers in a redox reaction (Mu *et al.*, 2015). In general, the coarse surface can increase the specific surface area of kapok fiber and improve the adhesion of fluid to the surface (Wang *et al.*, 2012). The particles on the surface of modified carbon fiber are a result of MnO₂ precipitation from the solution (Wang *et al.*, 2014). For sintered products, the Fig. 1d-f shows that the modified kapok carbon fiber remained intact and became spread and chaotically inserted in the sintered products. The sintered products prepared at 500°C exhibit more densely packed crystals than the ones made at sintering temperatures of 600 and 700°C. The images show porous structures with open voids, which become more prominent with increasing sintering temperature (Fig. 1e and 1f). The images also exhibit many broken kapok carbon fiber pieces with different sizes distributed irregularly in the sintered products prepared at 700°C. This is because during sintering at 700°C the rate and magnitude of total shrinkage are significantly increased (Bouziadi *et al.*, 2016). In addition, the different extent of shrinkage of mineral clays and modified kapok carbon fibers is due to their separation from each other (Velasco *et al.*, 2015). This phenomenon can result in the creation of tension and breakage (Ukwatta *et al.*, 2016). Thus, the sintered products prepared at 700°C are highly cracked and unsuitable for the testing of mechanical properties. These results show that sintering temperature of 700°C and addition of 60 wt% modified kapok carbon fiber are unsuitable conditions under which it is possible to avoid weakening of the mixture of raw materials during sintering. For further experiments the sintered product prepared with 40 wt% KMnO₄ modified kapok carbon fiber and sintered at 600°C (number 2) was used.

Effect of Contact Time for Fe³⁺ Ion Adsorption

The effect of contact time on Fe³⁺ ion removal at pH 7 by sintered filter made with 40 wt% KMnO₄ modified kapok carbon fiber and sintered filter made with 40 wt% kapok carbon fiber, both sintered at 600°C, is shown in Fig. 2. It was observed that the equilibrium time for Fe³⁺ ion removal was reached within 40 min for both the sintered filter with KMnO₄ modified kapok carbon fiber and the sintered filter with kapok carbon fiber. The KMnO₄ modified kapok carbon fiber filter could adsorb Fe³⁺ about 96%. It can be seen that Fe³⁺ adsorption efficiency of sintered filter with KMnO₄ modified kapok carbon fiber is higher than for the sintered filter with kapok carbon fiber by about 5-6% at equilibrium time. These results show that the KMnO₄ modification of kapok carbon fibers has an effect on Fe³⁺ adsorption. This is attributed to the specific chemisorptions of Fe³⁺ ions on the KMnO₄ modified kapok carbon fiber surfaces

(Tiwari *et al.*, 2011). However, Fe³⁺ began to precipitate at pH > 5 (He *et al.*, 2014). So, the Fe³⁺ ions may be removed by both adsorption and precipitation process. The precipitate was filtered by the sieve filtering process of the sintered filters. This experiment also showed that the Fe³⁺ ion concentration in the solution at equilibrium stage is 0.21 mg L⁻¹, which is lower than the drinking water standard value (0.3 mg L⁻¹) of TIS257-2549 (2006).

As shown in Fig. 3 and 4, the correlation coefficient (R^2) obtained from the Langmuir isotherm model (0.9976) is higher than the one for the Freundlich isotherm model (0.879) for Fe³⁺ adsorption by 40 wt% KMnO₄ modified kapok carbon fiber filter. Therefore, the Langmuir equation better represents the Fe³⁺ adsorption processes. It can be concluded that all sites on the sintered filter possess equal affinity for the Fe³⁺ ions in a monolayer adsorption process without interaction between Fe³⁺ ions and no transmigration (Liu *et al.*, 2013). The dimensionless separation parameter value (R_L), which was calculated using equation $R_L = 1/(1 + K_L C_0)$ (Sonmezay *et al.*, 2012), for the Fe³⁺ adsorption process is 0.245. This value lies in the range $0 < R_L < 1$, which indicates that the Fe³⁺ adsorption process by 40 wt% KMnO₄ modified kapok carbon fiber filter was favorable. The maximum adsorption capacity for Fe³⁺ ions of KMnO₄ modified kapok carbon fiber filter was calculated to be 53.76 mg g⁻¹ from the Langmuir plots. In comparison, the KMnO₄ modified pineapple leaf carbon fiber adsorbs Fe³⁺ with a capacity of only 25.25 mg g⁻¹ (Mopoung and Bunterm, 2016a). It was shown that the clay minerals also affect the efficiency of Fe³⁺ ions removal. The minerals consist of layers of two tetrahedral silica sheets sandwiching one octahedral alumina sheet and they have a permanent negative charge caused by the isomorphous substitution of Al³⁺ for Si⁴⁺ in the tetrahedral layer and metal ions for Al³⁺ in the octahedral layer. This negative charge is balanced by the presence of exchangeable cations in the lattice structure, which enables its good performance in adsorbing cationic contaminants by cationic exchange (Ma *et al.*, 2012). Moreover, the Fe³⁺ ion solution and precipitate can penetrate into the large apertures and channels of clay minerals (both zeolite and bentonite) (Ostroski *et al.*, 2009; Ma *et al.*, 2012) and kapok lumens of modified kapok carbon fiber filter without pronounced steric problems (Ostroski *et al.*, 2009). These phenomena result in highly effective Fe³⁺ ion removal. These experiments also confirmed that the Fe³⁺ ion concentrations in solution at equilibrium stage for all dosages of filters are in the range of 0.165-0.229 mg L⁻¹ which are lower than the drinking water standard value based on TIS257-2549.

Table 2. The linear drying shrinkage of wetted materials, linear firing shrinkage and density of sintered products

Number	% Drying shrinkage	% Firing shrinkage			Density (g/mL)		
		500°C	600°C	700°C	500°C	600°C	700°C
1	4.63	-	-	-	-	-	-
2	4.27	6	8	-	0.47	0.50	-
3	4.13	10	14	-	0.78	0.85	-
4	4.50	5	18	-	0.36	0.42	-

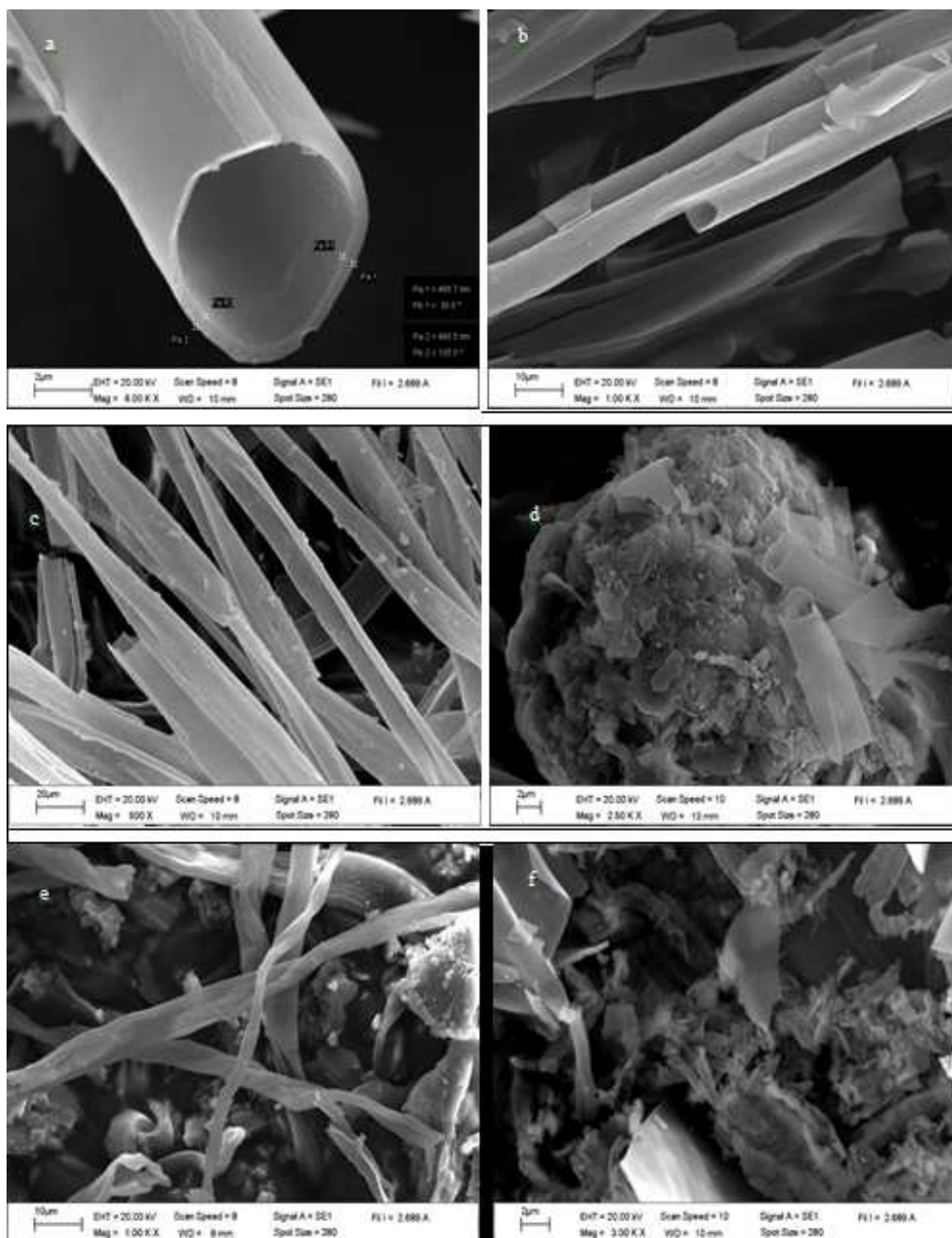


Fig. 1. The morphology structures of (a-b) kapok carbon fiber (c) KMnO_4 modified kapok carbon fiber (d) sintered filter with 40 wt% modified carbon prepared at 500°C (e) sintered filter 40 wt% modified carbon fiber prepared at 600°C and (f) sintered filter 40 wt% modified carbon fiber prepared at 700°C

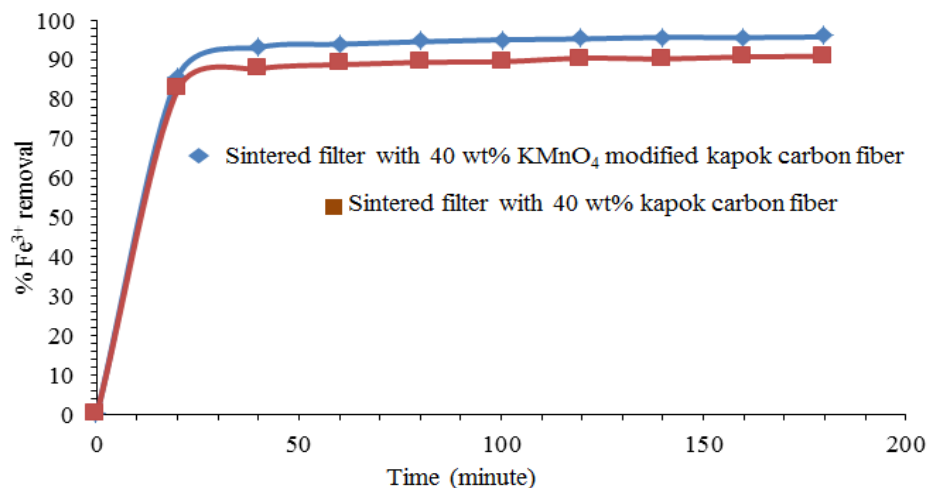


Fig. 2. Equilibrium time for Fe³⁺ ion removal by sintered product made with 40 wt% KMnO₄ modified kapok carbon fiber and sintered product with 40 wt% kapok carbon fibers sintered at 600°C

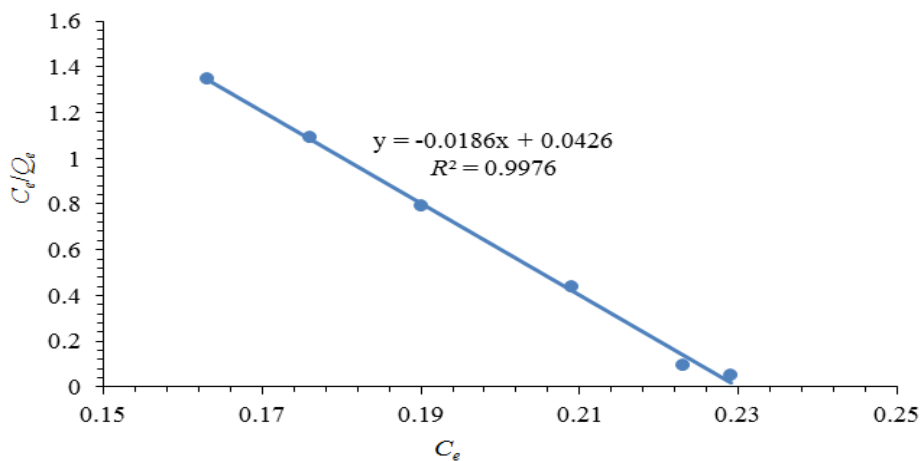


Fig. 3. Langmuir isotherm of Fe³⁺ adsorption by 40 wt% KMnO₄ modified kapok carbon fiber filters sintered at 600°C

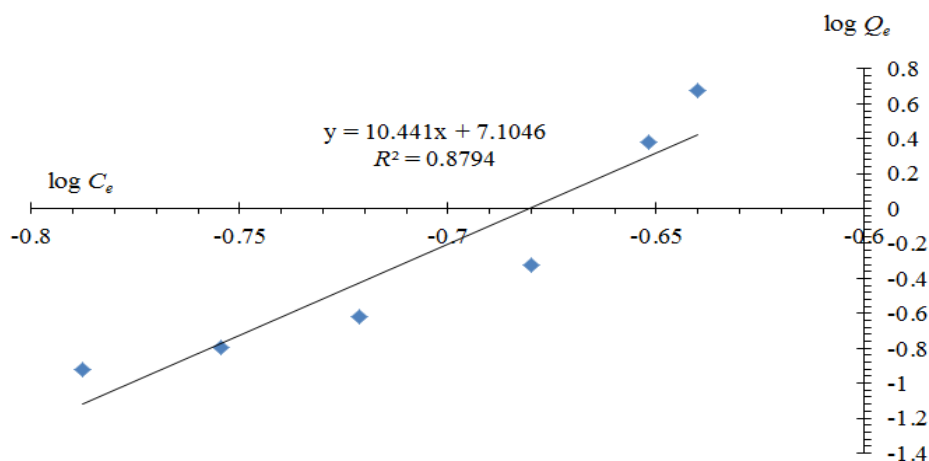


Fig. 4. Freundlich isotherm of Fe³⁺ adsorption by 40 wt% KMnO₄ modified kapok carbon fiber filters sintered at 600°C

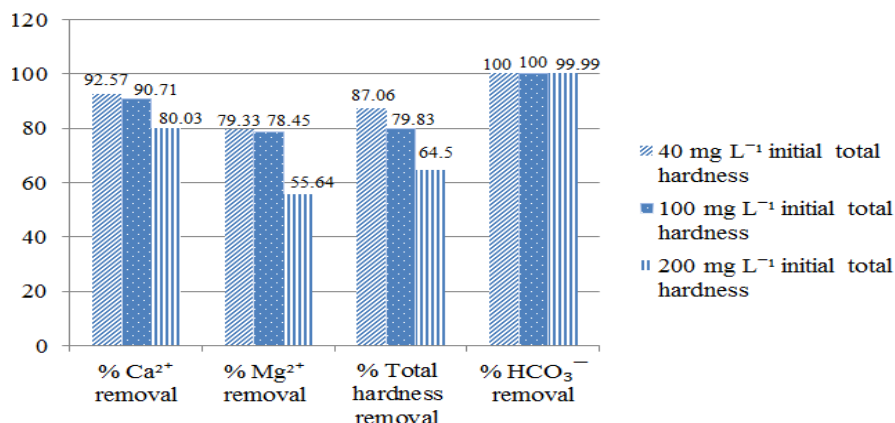


Fig. 5. Ca²⁺, Mg²⁺ and HCO₃⁻ ions removal efficiencies for initial total hardness of 40, 100 and 200 mg L⁻¹ by filter with 40 wt% KMnO₄ modified kapok carbon fibers sintered at 600°C

Efficiency of Ca²⁺, Mg²⁺ and HCO₃⁻ Adsorption

Figure 5 shows that the Ca²⁺, Mg²⁺ and total hardness removal efficiencies decrease with increasing initial total hardness concentrations. However, the HCO₃⁻ removal efficiencies remain nearly 100% for all initial total hardness concentrations. This decrease in the metal ion adsorption efficiencies with increasing initial total hardness concentrations for adsorption on modified kapok carbon fiber filter is possibly due to less active sites being available at equilibrium stage and the difficulty of the edge metal ions in penetrating the filter, due to metal ions partially covering the surface sites (Awwad *et al.*, 2013). On the other hand, the Ca²⁺, Mg²⁺ and HCO₃⁻ ion removal capacities of modified kapok carbon fiber filter are increased with increasing the total hardness from 40 mg to 100 mg and 200 mg L⁻¹ as in the following order: 4.49, 10.98 and 19.21 mg g⁻¹ for Ca²⁺, 1.55, 3.37 and 5.31 mg g⁻¹ for Mg²⁺ and 28.1, 61.75 and, 123.5 mg g⁻¹ for HCO₃⁻, respectively. This can be explained by higher surface charge (either positive or negative) of the filters at a given solution pH in response to increasing water hardness and alkalinity (Pastrana-Martínez *et al.*, 2010). Furthermore, at lower ion concentrations, the ions have a large number adsorption sites available to them. As the concentration of the ions increases, the competition for adsorption sites becomes more fierce. In these conditions, unit mass of the adsorbent takes up significantly more ions in comparison to conditions with lower ion concentrations resulting in an increase in adsorption capacities (Bhattacharyya and Gupta, 2008). In comparison KMnO₄ modified pineapple leaf carbon fiber (Mopoung and Bunterm, 2016b) showed a maximum Ca²⁺ adsorption capacity of only 2.81 mg g⁻¹. It is also clear that the clay minerals also affect Ca²⁺, Mg²⁺ and HCO₃⁻ ion removal. The high HCO₃⁻ adsorption efficiency of HCO₃⁻ removal

(100%) is also noteworthy. This result shows that all of the HCO₃⁻ ions were removed from solution. It is possible that the HCO₃⁻ ions reacted with Ca²⁺ and Mg²⁺ ions resulting in the precipitation of calcium carbonate or dolomite (CaMg(CO₃)₂) from the solution (Hannam *et al.*, 2016). These precipitates were removed from the solution by sieve filtering process of the sintered filter. In another case, excess bicarbonate could produce OH⁻ groups which correspond to the alcoholic hydroxyls groups (Fiore *et al.*, 2016) on the surface of the modified filter. Thus, the HCO₃⁻ ions were almost completely removed and could not be found by titration measurement.

Conclusion

The results of this research show that the KMnO₄ modified kapok carbon fiber and sintering temperature have an important effect on the physical properties of the sintered products. The linear drying shrinkage percentages of mixtures of raw materials increase with increasing content of modified kapok carbon fiber due to the amount of water used for the mixing process. After sintering, the firing shrinkages of the sintered products increase with increasing sintering temperature for the same ratios of raw materials. However, the firing shrinkages and densities of sintered products decrease with increasing content of the modified kapok carbon fiber at constant sintering temperature. The results also indicate that sintering at 700°C and adding 60 wt% of modified kapok carbon fiber results in products unsuitable filter fabrication as these conditions lead to larger defects in the sintered products. On the other hand, the sintered products produced by sintering at 500°C and containing 30 wt% of modified carbon fiber possess a highly dense texture. Therefore, the sintered product made using 40 wt% KMnO₄ modified kapok carbon fiber with sintering at

600°C was used for experiments of contaminants removal. For Fe³⁺ removal, the equilibrium of the adsorption was reached within 40 min for sintered filters. It was shown that at equilibrium the KMnO₄ modified kapok carbon fiber filter could adsorb 5-6% more Fe³⁺ ions than kapok carbon fiber filter. The Fe³⁺ ions were removed by adsorption and precipitation processes. Moreover, it was also shown that the Fe³⁺ ion concentration in solution at equilibrium is 0.21 mg L⁻¹, which is lower than the drinking water standard value (0.3 mg L⁻¹) of the TIS257-2549. The Fe³⁺ adsorption processes on modified carbon fiber filter can be fitted with the Langmuir isotherm model with maximum adsorption capacity of 53.76 mg g⁻¹. In addition, the removal of Ca²⁺, Mg²⁺, total hardness and HCO₃⁻ by modified kapok carbon fiber filter was observed to take place with high efficiency. The Ca²⁺, Mg²⁺ and HCO₃⁻ ion removal capacities in solutions with total hardness of 40 mg, 100 mg and 200 mg L⁻¹ by modified kapok carbon fiber filter are 4.49, 10.98 and 19.21 mg g⁻¹ for Ca²⁺, 1.55, 3.37 and 5.31 mg g⁻¹ for Mg²⁺ and 28.1, 61.75 and 123.5 mg g⁻¹ for HCO₃⁻, respectively.

Acknowledgement

The authors would like to thank the Chemistry Department and Science laboratory center, Faculty of Science, Naresuan University for all support.

Funding Information

This work was financially supported by Faculty of Science, Naresuan University.

Author's Contributions

Sumrit Mopoung: Designed the research plan, organized the study and wrote of all paragraphs.

Kannika Thongdee, Kalaporn Parun, Suphakrit Benjattitmongkhon and Krit Jamtim: Co-researchers who have reported and analyzed data presented in this paper.

Ethics

This article is original and contains unpublished material. The corresponding author confirms that all of the other authors have read and approved the manuscript and no ethical issues are involved.

References

Awad, N.S., A.A. El-Zahhar, A.M. Fouda and H.A. Ibrahim, 2013. Removal of heavy metal ions from ground and surface water samples using carbons derived from date pits. *J. Environ. Chem. Eng.*, 1: 416-423. DOI: 10.1016/j.jece.2013.06.006

- Bhatnagar, A., W. Hogland, M. Marques and M. Sillanpää, 2013. An overview of the modification methods of activated carbon for its water treatment applications. *Chem. Eng. J.*, 219: 499-511. DOI: 10.1016/j.cej.2012.12.038
- Bhattacharyya, K.G. and S.S Gupta. 2008. Adsorption of Fe(III), Co(II) and Ni(II) on ZrO-kaolinite and ZrO-montmorillonite surfaces in aqueous medium. *Colloids Surfaces Physicochem. Eng. Aspects*, 317: 71-79. DOI: 10.1016/j.colsurfa.2007.09.037
- Boonamnuayvitaya, V., C. Chaiya, W. Tanthapanichakoon and S. Jarudilokkul. 2004. Removal of heavy metals by adsorbent prepared from pyrolyzed coffee residues and clay. *Separat. Purificat. Technol.*, 35: 11-22. DOI: 10.1016/S1383-5866(03)00110-2
- Bories, C., E. Vedrenne, A. Paulhe-Massol, G. Vilarem and C. Sablayrolles. 2016. Development of porous fired clay bricks with bio-based additives: Study of the environmental impacts by Life Cycle Assessment (LCA). *Constr. Build. Mater.*, 125: 1142-1151. DOI: 10.1016/j.conbuildmat.2016.08.042
- Bories, C., L. Aouba, E. Vedrenne and G. Vilarem. 2015. Fired clay bricks using agricultural biomass wastes: Study and characterization. *Constr. Build. Mater.*, 91: 158-163. DOI: 10.1016/j.conbuildmat.2015.05.006
- Bouziadi, F., B. Boulekbache and M. Hamrat, 2016. The effects of fibres on the shrinkage of high-strength concrete under various curing temperatures. *Constr. Build. Mater.*, 114: 40-48. DOI: 10.1016/j.conbuildmat.2016.03.164
- Chaturvedi, S. and P.N. Dave. 2012. Removal of iron for safe drinking water. *Desalination*, 303: 1-11. DOI: 10.1016/j.desal.2012.07.003
- Chung, J.T., K.J. Hwang, W.G. Shim, C. Kim and J.Y. Park *et al.*, 2013. Synthesis and characterization of activated hollow carbon fibers from *Ceiba pentandra* (L.) Gaertn. (kapok). *Mater. Lett.*, 93: 401-403. DOI: 10.1016/j.matlet.2012.09.016
- Dong, T., F. Wang and G. Xu, 2015a. Sorption kinetics and mechanism of various oils into kapok assembly. *Marine Pollut. Bull.*, 91: 230-237. DOI: 10.1016/j.marpolbul.2014.11.044
- Dong, T., G. Xu and F. Wang, 2015b. Adsorption and adhesiveness of kapok fiber to different oils. *J. Hazardous Mater.*, 296: 101-111. DOI: 10.1016/j.jhazmat.2015.03.040
- Du, Y., G. Zheng, J. Wang, L. Wang and J. Wu *et al.*, 2014. MnO₂ nanowires in situ grown on diatomite: Highly efficient absorbents for the removal of Cr(VI) and As(V). *Microporous Mesoporous Mater.*, 200: 27-34. DOI: 10.1016/j.micromeso.2014.07.043

- Eliche-Quesada, D., M.A. Felipe-Sesé, J.A. López-Pérez and A. Infantes-Molina, 2017. Characterization and evaluation of rice husk ash and wood ash in sustainable clay matrix bricks. *Ceram. Int. Part A*, 43: 463-475. DOI: 10.1016/j.ceramint.2016.09.181
- Fang, L., R. Hong, J. Gao and C. Gu, 2016. Degradation of bisphenol A by nano-sized manganese dioxide synthesized using montmorillonite as templates. *Applied Clay Sci.*, 132-133: 155-160. DOI: 10.1016/j.clay.2016.05.028
- Fiore, V., T. Scalici, F. Nicoletti, G. Vitale and M. Prestipino *et al.*, 2016. A new eco-friendly chemical treatment of natural fibres: Effect of sodium bicarbonate on properties of sisal fibre and its epoxy composites. *Comp. Part B*, 85: 150-160. DOI: 10.1016/j.compositesb.2015.09.028
- Fujiwara, K., T. Masubuchi, K. Miyata, M. Shiozawa and T. Takato *et al.*, 2010. Metal oxides immobilized fabrics by radiation induced graft polymerization. *Radiat. Phys. Chem.*, 79: 238-240. DOI: 10.1016/j.radphyschem.2009.08.035
- Görhan, G. and O. Şimşek, 2013. Porous clay bricks manufactured with rice husks. *Constr. Build. Mater.*, 40: 390-396. DOI: 10.1016/j.conbuildmat.2012.09.110
- Hajji, L., A. Boukir, J. Assouik, S. Pessanha and J.L. Figueirinhas *et al.*, 2016. Artificial aging paper to assess long-term effects of conservative treatment. Monitoring by infrared spectroscopy (ATR-FTIR), X-Ray Diffraction (XRD) and Energy Dispersive X-Ray Fluorescence (EDXRF). *Microchem. J.*, 124: 646-656. DOI: 10.1016/j.microc.2015.10.015
- Han, Q., W. Dong, H. Wang, T. Liu and F. Sun *et al.*, 2013. Effects of coexisting anions on decolorization of azo dye X-3B by ferrate (VI) and a comparative study between ferrate (VI) and potassium permanganate. *Separat. Purificat. Technol.*, 108: 74-82. DOI: 10.1016/j.seppur.2013.01.053
- Hannam, K.D., D. Kehila, P. Millard, A.J. Midwood and D. Neilsen *et al.*, 2016. Bicarbonates in irrigation water contribute to carbonate formation and CO₂ production in orchard soils under drip irrigation. *Geoderma*, 266: 120-126. DOI: 10.1016/j.geoderma.2015.12.015
- He, Z., H. Song, Y. Cui, W. Zhu and K. Du *et al.*, 2014. Porous spherical cellulose carrier modified with polyethyleneimine and its adsorption for Cr(III) and Fe(III) from aqueous solutions. *Chinese J. Chem. Eng.*, 22: 984-990. DOI: 10.1016/j.cjche.2014.07.001
- Kinuthia, J.M. and J.E. Oti, 2012. Designed non-fired clay mixes for sustainable and low carbon use. *Applied Clay Sci.*, 59-60: 131-139. DOI: 10.1016/j.clay.2012.02.021
- Koshy, N. and D.N. Singh, 2016. Fly ash zeolites for water treatment applications. *J. Environ. Chem. Eng.*, 4: 1460-1472. DOI: 10.1016/j.jece.2016.02.002
- Leboda, R., S. Chodorowski, J. Skubiszewska-Zięba and Y.I. Tarasevich, 2001. Effect of the carbonaceous matter deposition on the textural and surface properties of complex carbon-mineral adsorbents prepared on the basis of palygorskite. *Colloids Surfaces Physicochem. Eng. Aspects*, 178: 113-128. DOI: 10.1016/S0927-7757(00)00587-2
- Li, Z.S., H.Q. Wang, Y.G. Huang, Q.Y. Li and X.Y. Wang, 2010. Manganese dioxide-coated activated mesocarbon microbeads for supercapacitors in organic electrolyte. *Colloids Surfaces Physicochem. Eng. Aspects*, 366: 104-109. DOI: 10.1016/j.colsurfa.2010.05.031
- Lin, T., L. Li, W. Chen and S. Pan, 2012. Effect and mechanism of preoxidation using potassium permanganate in an ultrafiltration membrane system. *Desalination*, 286: 379-388.
- Liu, J., X. Gao, C. Liu, L. Guo and S. Zhang *et al.*, 2013. Adsorption properties and mechanism for Fe(III) with solvent impregnated resins containing HEHEHP. *Hydrometallurgy*, 137: 140-147.
- Liu, Y., J. Wang, Y. Zheng and A. Wang, 2012. Adsorption of methylene blue by kapok fiber treated by sodium chlorite optimized with response surface methodology. *Chem. Eng. J.*, 184: 248-255.
- Loiola, A.R., J.C.R.A. Andrade, J.M. Sasaki and L.R.D. da Silva, 2012. Structural analysis of zeolite NaA synthesized by a cost-effective hydrothermal method using kaolin and its use as water softener. *J. Colloid Interface Sci.*, 367: 34-39.
- Lu, Z., T. Lin, W. Chen and X.B. Zhang, 2015. Influence of KMnO₄ preoxidation on ultrafiltration performance and membrane material characteristics. *J. Membrane Sci.*, 486: 49-58.
- Lyra, F.H., M.T.W.D. Carneiro, G.P. Brandão, H.M. Pessoa and E.V. de Castro, 2010. Determination of Na, K, Ca and Mg in biodiesel samples by flame Atomic Absorption Spectrometry (FAAS) using microemulsion as sample preparation. *Microchem. J.*, 96: 80-185.
- Ma, J., J. Qi, C. Yao, B. Cui and T. Zhang *et al.*, 2012. A novel bentonite-based adsorbent for anionic pollutant removal from water. *Chem. Eng. J.*, 200-202: 97-103. DOI: 10.1016/j.cej.2012.06.014
- McLaughlan, R.G., S.M.G. Hossain and O.A. Al-Mashaqbeh, 2015. Zinc sorption by permanganate treated pine chips. *J. Environ. Chem. Eng.*, 3: 1539-1545. DOI: 10.1016/j.jece.2015.05.022
- Monteiro, S.N. and C.M.F. Vieira, 2004. Influence of firing temperature on the ceramic properties of clays from Campos dos Goytacazes, Brazil. *Applied Clay Sci.*, 27: 229-234.
- Mopoung, S. and P. Amornsakchai, 2016. Microporous activated carbon fiber from pineapple leaf fiber by H₃PO₄ activation. *Asian J. Scientific Res.*, 9: 24-33. DOI: 10.3923/ajsr.2016.24.33

- Mopoung, S. and T. Bunterm, 2016a. KMnO₄ modified carbon prepared from waste of pineapple leaf fiber production processing for removal of ferric ion from aqueous solution. *Am. J. Applied Sci.*, 13: 814-826. DOI: 10.3844/ajassp.2016.814.826
- Mopoung, S. and T. Bunterm, 2016b. Calcium ion removal by KMnO₄ modified pineapple leaf waste carbon prepared from waste of pineapple leaf fiber production processing. *Carbon Sci. Technol.*, 8: 13-19.
- Morales-Pinzón, T., R. Lurueña, X. Gabarrell, C.M. Gasol and J. Rieradevall, 2014. Financial and environmental modelling of water hardness-Implications for utilising harvested rainwater in washing machines. *Sci. Total Environ.*, 470-471: 1257-1271. DOI: 10.1016/j.scitotenv.2013.10.101
- Mu, B., W.B. Zhang and W.B. Xu, 2015. Hollowed-out tubular carbon@MnO₂ hybrid composites with controlled morphology derived from kapok fibers for supercapacitor electrode materials. *Electrochim. Acta*, 178: 709-720. DOI: 10.1016/j.electacta.2015.08.091
- Ostroski, I.C., M.A.S.D. Barros, E.A. Silva, J.H. Dantas and P.A. Arroyoamnd *et al.*, 2009. A comparative study for the ion exchange of Fe(III) and Zn(II) on zeolite NaY. *J. Hazard. Mater.*, 161: 1404-1412. DOI: 10.1016/j.jhazmat.2008.04.111
- Pastrana-Martínez, L.M., M.V. López-Ramón, M.A. Fontecha-Cámara and C. Moreno-Castilla, 2010. Batch and column adsorption of herbicide fluroxypyr on different types of activated carbons from water with varied degrees of hardness and alkalinity. *Water Res.*, 44: 879-885. DOI: 10.1016/j.watres.2009.09.053
- Pawar, R.R., Lalmunsiana, H.C. Bajaj and S.M. Lee, 2016. Activated bentonite as a low-cost adsorbent for the removal of Cu(II) and Pb(II) from aqueous solutions: Batch and column studies. *J. Indust. Eng. Chem.*, 34: 213-223. DOI: 10.1016/j.jiec.2015.11.014
- Rasheed, A., J.Y. Howe, M.D. Dadmun and P.F. Britt, 2007. The efficiency of the oxidation of carbon nanofibers with various oxidizing agents. *Carbon*, 45: 1072-1080. DOI: 10.1016/j.carbon.2006.12.010
- Reddy, N. and Y. Yang, 2005. Biofibers from agricultural byproducts for industrial applications. *TRENDS Biotechnol.*, 23: 22-27. DOI: 10.1016/j.tibtech.2004.11.002
- Sonmezay, A., M. Salimoncel and N. Bektas, 2012. Adsorption of lead and cadmium ions from aqueous solutions using manganoxide minerals. *Trans. Nonferrous Metals Society China*, 22: 3131-3139. DOI: 10.1016/S1003-6326(12)61765-8
- Sultanbayeva, G.S., R. Holze, R.M. Chernyakova and U.Z. Jussipbekov, 2013. Removal of Fe²⁺, Cu²⁺, Al³⁺ and Pb²⁺ ions from phosphoric acid by sorption on carbonate-modified natural zeolite and its mixture with bentonite. *Microporous Mesoporous Mater.*, 170: 173-180. DOI: 10.1016/j.micromeso.2012.11.022
- Tahir, S.S. and R. Naseem, 2007. Removal of Cr(III) from tannery wastewater by adsorption onto bentonite clay. *Separat. Purificat. Technol.*, 53: 312-321. DOI: 10.1016/j.seppur.2006.08.008
- Tian, M., M. Du, L. Qu, K. Zhang and H. Li *et al.*, 2016. Conductive reduced graphene oxide/MnO₂ carbonized cotton fabrics with enhanced electrochemical, -heating and -mechanical properties. *J. Power Sources*, 326: 428-437.
- TIS257-2549, 2006. Thai Industrial Standard Institute, Ministry of industry, Drinking water.
- Tiwari, D., C. Laldanwngliana, C.H. Choi and S.M. Lee, 2011. Manganese-modified natural sand in the remediation of aquatic environment contaminated with heavy metal toxic ions. *Chem. Eng. J.*, 171: 958-966.
- Üçer, A., A. Uyanık, S. Çay and Y. Özkan, 2005. Immobilisation of tannic acid onto activated carbon to improve Fe(III) adsorption. *Separat. Purificat. Technol.*, 44: 11-17.
- Uddin, M.K., 2017. A review on the adsorption of heavy metals by clay minerals, with special focus on the past decade. *Chem. Eng. J.*, 308: 438-462.
- Ukwatta, A., A. Mohajerani, N. Eshtiaghi and S. Setunge, 2016. Variation in physical and mechanical properties of fired-clay bricks incorporating ETP biosolids. *J. Cleaner Product.*, 119: 76-85. DOI: 10.1016/j.jclepro.2016.01.094
- van Garderen, N., F.J. Clemens, M. Mezzomo, C.P. Bergmann and T.T. Graule, 2011. Investigation of clay content and sintering temperature on attrition resistance of highly porous diatomite based material. *Applied Clay Sci.*, 52: 115-121. DOI: 10.1016/j.clay.2011.02.008
- Velasco, P.M., M.P.M. Ortiz, M.A.M. Giró, D.M. Melia and J.H. Rehbein, 2015. Development of sustainable fired clay bricks by adding kindling from vine shoot: Study of thermal and mechanical properties. *Applied Clay Sci.*, 107: 156-164.
- Vilaplana, J.L., F.J. Baeza, O. Galao, E.G. Alcocel and E. Zornoza *et al.*, 2016. Mechanical properties of alkali activated blast furnace slag pastes reinforced with carbon fibers. *Construct. Build. Mater.*, 116: 63-71. DOI: 10.1016/j.conbuildmat.2016.04.066
- Wang, J., G. Geng, X. Liu, F. Han and J. Xu, 2016. Magnetically superhydrophobic kapok fiber for selective sorption and continuous separation of oil from water. *Chem. Eng. Res. Design*, 115: 122-130. DOI: 10.1016/j.cherd.2016.09.032
- Wang, J., Y. Zheng, Y. Kang and A. Wang, 2013. Investigation of oil sorption capability of PBMA/SiO₂ coated kapok fiber. *Chem. Eng. J.*, 223: 632-637. DOI: 10.1016/j.cej.2013.03.007
- Wang, J., Y. Zheng and A. Wang, 2012. Effect of kapok fiber treated with various solvents on oil absorbency. *Indust. Crops Prod.*, 40: 178-184.

- Wang, M., H. Liu, Z.H. Huang and F. Kang, 2014. Activated carbon fibers loaded with MnO₂ for removing NO at room temperature. *Chem. Eng. J.*, 256: 101-106. DOI: 10.1016/j.cej.2014.06.108
- Wu, Z., L. Sun and J. Wang, 2016. Synthesis and characterization of porous Y₂SiO₅ with low linear shrinkage, high porosity and high strength. *Ceram. Int.*, 42: 14894-14902. DOI: 10.1016/j.ceramint.2016.06.128
- Xuwen, H., Y. Huimin and H. Yong, 2010. Treatment of mine water high in Fe and Mn by modified manganese sand. *Min. Sci. Technol.*, 20: 571-575. DOI: 10.1016/S1674-5264(09)60246-5
- Ye, H. and A. Radlińska, 2016. Shrinkage mechanisms of alkali-activated slag. *Cement Concrete Res.*, 88: 126-135. DOI: 10.1016/j.cemconres.2016.07.001
- Zarei-Baygi, A., M. Moslemi and S.H. Mirzaei, 2016. The combination of KMnO₄ oxidation and polymeric flocculation for the mitigation of membrane fouling in a membrane bioreactor. *Separat. Purificat. Technol.*, 159: 124-134. DOI: 10.1016/j.seppur.2016.01.003
- Zheng, Y., J. Wang, Y. Zhu and A. Wang, 2015. Research and application of kapok fiber as an absorbing material: A mini review. *J. Environ. Sci.*, 27: 21-32. DOI: 10.1016/j.jes.2014.09.026